Infrared Flux Divergence Calculations with Newly Constructed Radiation Tables[1]

WILFORD G. ZDUNKOWSKI AND FRANK G. JOHNSON, CAPTAIN, USAF
University of Utah, Salt Lake City

(Manuscript received 25 September 1964, in revised form 10 December 1964)

ABSTRACT

This paper presents some sample computations of infrared radiative flux divergence due to atmospheric water vapor. These calculations are based upon newly constructed radiation tables which were obtained from the radiometersonde observations of P. M. Kuhn. The results are compared with the findings of other investigators. The importance of the surface-air temperature discontinuity is demonstrated.

1. Introduction

Among the basic problems in meteorology is the determination of the atmospheric heat budget since it has long been recognized that the difference between the short-wave radiation absorbed by the earth-atmosphere complex and the long-wave radiation to space constitutes the atmospheric heat engine. Radiative temperature changes are due to radiative flux divergence, a quantity which can be computed only after laborious manipulations involving the vertical temperature and moisture gradients. Although these temperature changes are usually too slow in the free atmosphere to play an important role in daily synoptic changes, they constitute a process that goes on continually. Therefore, attempts are being made to incorporate this non-adiabatic effect into numerical forecasting models.

Near clouds and near the surface of the earth, the radiative energy contribution is extremely important. Möller (1951) has shown, for example, the importance of radiative cooling in cloud destabilization. His and other radiation diagrams and tables in use today are based upon simplified versions of the spectrum. In addition, absorption data contained in these charts have been obtained in the laboratory, where conditions of varying temperature, pressure, and moisture as observed in the atmosphere can be simulated only imperfectly. Such simplifications are not contained in our new radiation tables.

Brooks (1950) proposed a tabular method for the computation of flux divergence which offers the advantage of finding radiative temperature changes with relative ease. The method requires a knowledge of the quantity $\Delta\epsilon/\Delta X$ which is the finite difference slope of the emissivity curve ϵ as a function of the gaseous optical depth X. His emissivity curve is based in part on laboratory measurements, supplemented by data obtained from downward flux measurements at the earth's surface. However, Kuhn (1963) has taken flux measurements in the free atmosphere and has constructed a water vapor emissivity curve based on these new data. The authors, following Brooks, have taken this curve and constructed new radiation tables[2] which may well replace or supplement Brooks' older data. In addition, the new slope tables include water vapor path lengths as small as 10^{-5} cm which are not found in the older tables. Their use in micrometeorological work is obvious. Ozone and carbon dioxide effects have not been taken into consideration.

2. Data and compilation of tables

Details about the acquisition of Kuhn's emissivity data are given elsewhere (Kuhn, 1963). He found, when calculating infrared radiative flux in the atmosphere, that a pressure-reduced optical depth of $(p/p_0)^{0.85}$ would improve accuracy. His method, however, was not delicate enough to obtain experimental data on the temperature dependence of the emissivity function. Judged by Yamamoto's (1953) radiation chart, such a temperature dependency will be very small for temperatures normally found in the troposphere and may be altogether neglected in micrometeorological work. A further advantage of using Kuhn's data is found in the fact that he actually observed hemispheric radiation, while Brooks multiplied his path-length values by 1.66 to convert from beam to flux emissivities.

In order to maintain a smooth transition between the given data points, it was necessary for the slope computations to change some of the original emissivity values. In no case did these changes amount to more than one

[1] This research was sponsored in part by National Science Foundation, Grant GP-647.

[2] Due to the fact that the new radiation tables are somewhat extensive, it is impossible to include them in this publication. Interested persons may obtain them at cost price through the Department of Meteorology of the University of Utah.

per cent of the given values. It should be noted that such changes were made only in regions where the emissivity values were large. The quantity $\Delta\epsilon/\Delta X$ was then obtained from large scale graphs. Only minor adjustments were required as detailed plots of the slope curves have indicated. Emissivities for path lengths smaller than 0.0001 cm of ppw were not obtained from measurements but have been estimated from the following equation:

$$\epsilon = a \log_{10}(1+bX). \tag{1}$$

The constants "a" and "b" assume the values 0.11288 and 12.635 cm^{-1}, respectively. This equation meets the required boundary condition for the interval of approximation; i.e., when $X=0$, $\epsilon=0$. Table 1 shows

TABLE 1. Comparison of emissivity values.

X	ϵ, Kuhn	ϵ, Formula	Relative Error
0.001	0.1280	0.1280	0
0.0003	0.0780	0.0767	−1.6%
0.0001	0.0400	0.0400	0

a comparison of emissivity values obtained from Kuhn's basic data and by means of the above formula for some of the smaller values of optical path length. Thus, the correct shape of the emissivity curve has been taken into account. To insure proper continuity from the given to the computed tables, values derived from this formula were checked against values obtained from a graphical extension to an optical depth of 0.00005 cm.

Values from 3.0 cm to 5 cm of water were obtained by straight-line extrapolation, a correct technique due to the flatness of the curve. A comparison of the adopted emissivity data (labeled Kuhn) with values given by other authors is made in Table 2. Table 2 shows that the extrapolated value after Eq. (1) is significantly higher than corresponding extrapolations by Hales *et al.* (1963) using Brooks' original data and by Möller and Zdunkowski (1962) extrapolation using Möller's original data.

3. Theoretical basis for calculations

The new radiation tables will be applied to some interesting cases. The computational method selected is described by Hales, Zdunkowski and Henderson (1964) who have generalized Brooks' formula such that spectral overlap effects of water vapor with haze, and other gases may be taken into consideration. Moreover, the generally observed temperature discontinuity at the air-surface interface can be taken into account. Brooks' method does not offer these possibilities. According to Hales, Zdunkowski and Henderson (1964) the flux divergence at the level Z' is given by:

$$\frac{dS(Z')}{dZ'} = \left[B(\infty)\frac{d\tau}{dZ'}\right] - \int_{B(0)}^{B(\infty)} \frac{d\tau}{dZ'} dB + [B(G)-B(0)]\left[\frac{d\tau}{dZ'}\right] \tag{2}$$

if the transmission function is denoted by τ. Here $B(Z)$ stands for the black body radiation evaluated at the levels $Z=0$, the surface of the earth, and $Z=\infty$ (the effective radiative top of the atmosphere), while dB is evaluated according to a given atmospheric sounding. Infinity is a relative concept. Due to the small amount of water vapor present in the stratosphere, the change of $d\tau/dX$ is small above the tropopause. Therefore, in micrometeorological studies, $B(\infty)$ may be evaluated using the temperature observed at the tropopause. $B(G)$ is evaluated using the temperature of the surface of the earth, while $B(0)$ stands for the black body radiation evaluated at the temperature of the air directly overlying the ground. An equivalent interpretation is valid for $d\tau/dZ'$. τ, the total transmission in Eq. (2), may be expressed as a product of individual transmissions of atmospheric gases and haze. Since water vapor is the only gas to be considered, τ is then the transmission factor for this gas. The following identity is self-evident:

$$\frac{d\tau}{dZ'} = \frac{d\tau}{dX}\frac{dX}{dZ'}. \tag{3}$$

Here X is an absolute value function as defined in terms of the water vapor path length w, evaluated from the top of the atmosphere by

$$X = |w-w'|, \tag{4}$$

where w' is the path length at the reference level. Denoting the pressure corrected specific humidity by q and the density of the air by ρ_a,

$$dw = -q\rho_a dZ. \tag{5}$$

TABLE 2. Emissivity.

X (cm)		10^{-5}	10^{-4}	10^{-3}	10^{-2}	10^{-1}	1	5
Kuhn (1963)		0.0058	0.0400	0.128	0.249	0.381	0.543	0.618
Elsasser (1960)	($T=10$)		0.0500	0.140	0.280	0.410	0.540	0.630
Yamamoto (1953)			0.0270	0.093	0.215	0.393	0.622	
Brooks (1953)		0.0029	0.0244	0.116	0.246	0.396	0.575	0.702
Möller and Zdunkowski (1962)	($T=-20$)	0.0037	0.0280	0.135	0.326	0.500	0.630	0.723
	($T=20$)	0.0027	0.0247	0.115	0.289	0.454	0.595	0.704

Eq. (3) uses the following sign convention:

$$\begin{aligned} d\tau/dZ' &< 0 \text{ if } Z<Z' \\ d\tau/dZ' &> 0 \text{ if } Z>Z' \end{aligned} \tag{6}$$

Since τ always decreases with increasing path length and X is an absolute value function, it follows that $d\tau/dX$ is always negative. Hence:

$$\begin{aligned} dX/dZ' &> 0 \text{ if } Z<Z' \\ dX/dZ' &< 0 \text{ if } Z>Z'. \end{aligned} \tag{7}$$

The quantity dX/dZ' stands for the concentration of water vapor, $\rho_V(Z')$, at the reference level. Absolute values of $d\tau/dX$ and $\rho_V(Z')$ are introduced to eliminate all difficulties that may arise due to sign convention. Noting the relationship of emissivity and transmissivity as given by

$$\epsilon = 1-\tau \quad \text{and} \quad \left|\frac{d\epsilon}{dX}\right| = \left|\frac{d\tau}{dX}\right| \tag{8}$$

and using the sign convention of (7), Eq. (2) assumes the form,

$$\frac{dS(Z')}{dZ'} = |\rho_V(Z')| \left\{ B(\infty)\left|\frac{d\epsilon}{dX}\right|_\infty + \int_{B(0)}^{B(Z')} \left|\frac{d\epsilon}{dX}\right| dB - \int_{B(Z')}^{B(\infty)} \left|\frac{d\epsilon}{dX}\right| dB - [B(G)-B(0)]\left|\frac{d\epsilon}{dX}\right|_0 \right\}. \tag{9}$$

The quantity dB is always negative when the temperature decreases with height, and positive in the case of an inversion

The radiative temperature change with time at the level Z' is given by

$$\frac{dT}{dt} = -\frac{1}{\rho_a C_p}\frac{dS(Z')}{dZ'}, \tag{10}$$

where C_p stands for the specific heat at constant pressure. In finite difference form, (10) becomes

$$\frac{\Delta T}{\Delta t} = \frac{|q|}{C_p}\left\{ -B(\infty)\left|\frac{d\epsilon}{dX}\right|_\infty - \sum_{i=1}^{N}\left|\frac{\Delta\epsilon}{\Delta X}\right|\Delta B + \sum_{N}^{M}\left|\frac{\Delta\epsilon}{\Delta X}\right|\Delta B + [B(G)-B(0)]\left|\frac{d\epsilon}{dX}\right|_0 \right\} \tag{11}$$

where M stands for the total number of atmospheric layers considered, and N the number of layers below the reference level. M, B, q and X are determined by the given sounding. Therefore, $\Delta\epsilon/\Delta X$ can be obtained from the newly constructed slope tables. The instantaneous slopes, $d\epsilon/dX$ are found as headings of the slope tables, while the instantaneous slope, $d\epsilon(0)/dX$, if required may be obtained by differentiation of Eq. (1), i.e.,

$$\frac{d}{dX}[a\log_{10}(1+bX)] = 618.35 \text{ cm}^{-1}. \tag{12}$$

In the special case of no interface temperature discontinuity, Eq. (11) reduces to Brooks' formula.

4. Sample calculations

In order to have a comparison with results obtained by means of Brooks' table (1950) his sample computation was repeated using the path lengths furnished. The result is shown in Fig. 1 indicating that the new tables, with the exception at the surface, give somewhat smaller cooling rates. Kuhn's pressure correction, instead of the square root correction applied by Brooks, would yield only insignificant changes.

Fig. 2 shows a comparison of radiative temperature changes over Seabrook Farms, New Jersey, based upon Möller's and Zdunkowski's (1962) radiation tables and Brooks' extended radiation tables. The latter two were reported by Hales, Zdunkowski and Henderson (1964). This hypothetical sounding contains in the lower levels a model surface inversion with isothermal conditions above. At higher levels, the temperature and dew point curves are based on observed data at Seabrook Farms, N. J. A dew-point temperature of 16.5C was assumed to be constant with height in the lower few meters. In general, the new radiative cooling curve appears to be a good compromise between Möller's and Brooks' analyses.

Fig. 3a represents an analysis of the radiative cooling in a continental polar air mass. The data are based in the lower levels on a winter sounding under clear sky conditions at Vladivostok, USSR, as reported by Petterssen (1940); above 400 mb, the data were obtained from a U. S. Air Force manual (1955). The contribution of the interface temperature difference as before is neglected in the computation. As is expected from other investigations, cooling prevails through the 500-mb level. A decrease in specific humidity from 0.45 to 0.22 gm per kg between the 800- and 700-mb levels causes very ineffective screening of the net upward flux. The result is maximum radiative cooling at the 800-mb level. No low level inversion is present. In Fig. 3b, a very shallow surface inversion of 2.5C was introduced in the lower 300 cm without changing any basic data. Different results are obtained in the lower levels such as warming in the lower 160 cm and strong cooling at the 300-cm level. At greater heights, the cooling profile shown in Fig. 3a is approached.

Next, the instantaneous radiative temperature change occurring in the lower levels of a model continental tropical air mass will be investigated. The influence of the surface-air discontinuity will be studied also. The model was based on a 0000Z sounding of 31 August 1958, at Aswan, United Arab Republic (International

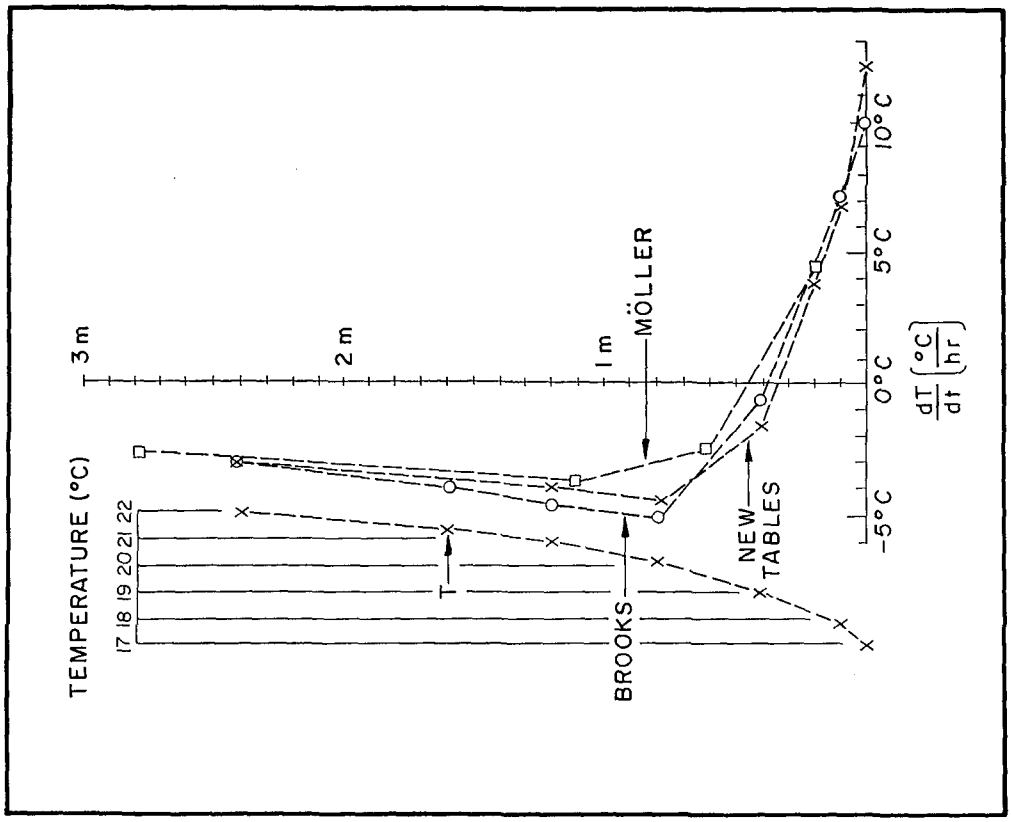

FIG. 2. A comparison of three emissivity curves used for computing radiative cooling, assuming a strong temperature inversion.

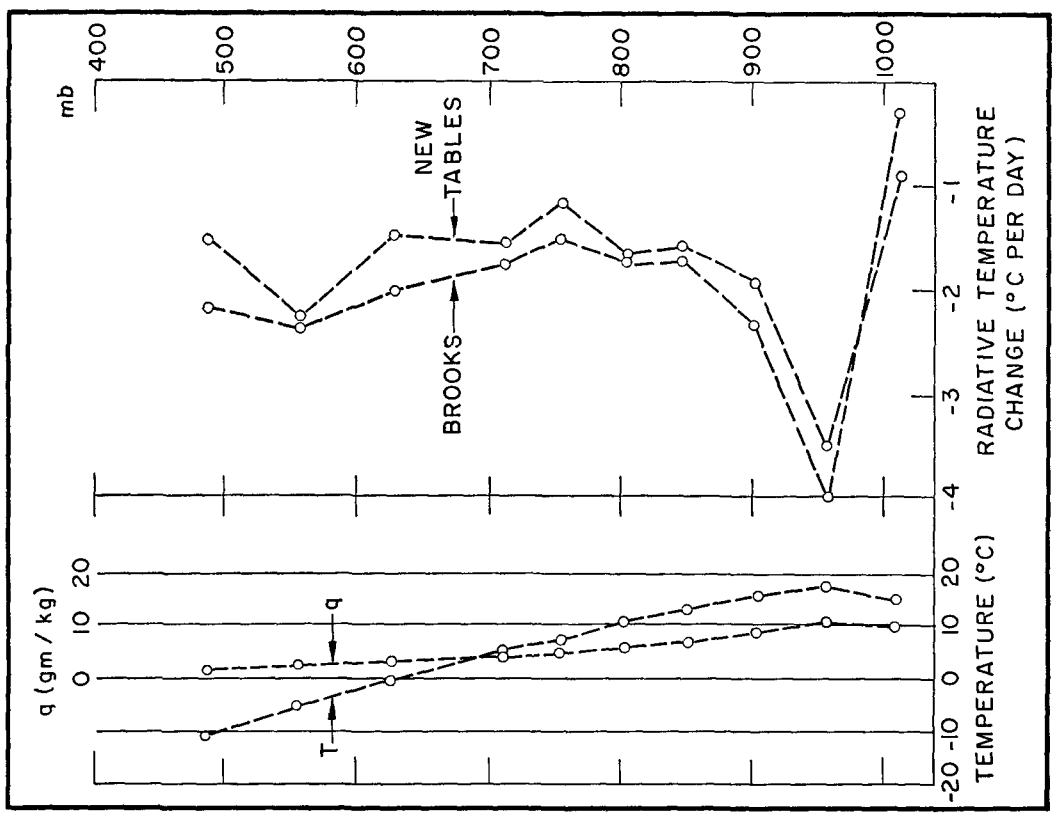

FIG. 1. Mean sounding and rate of temperature change, July 1941, Portland, Maine.

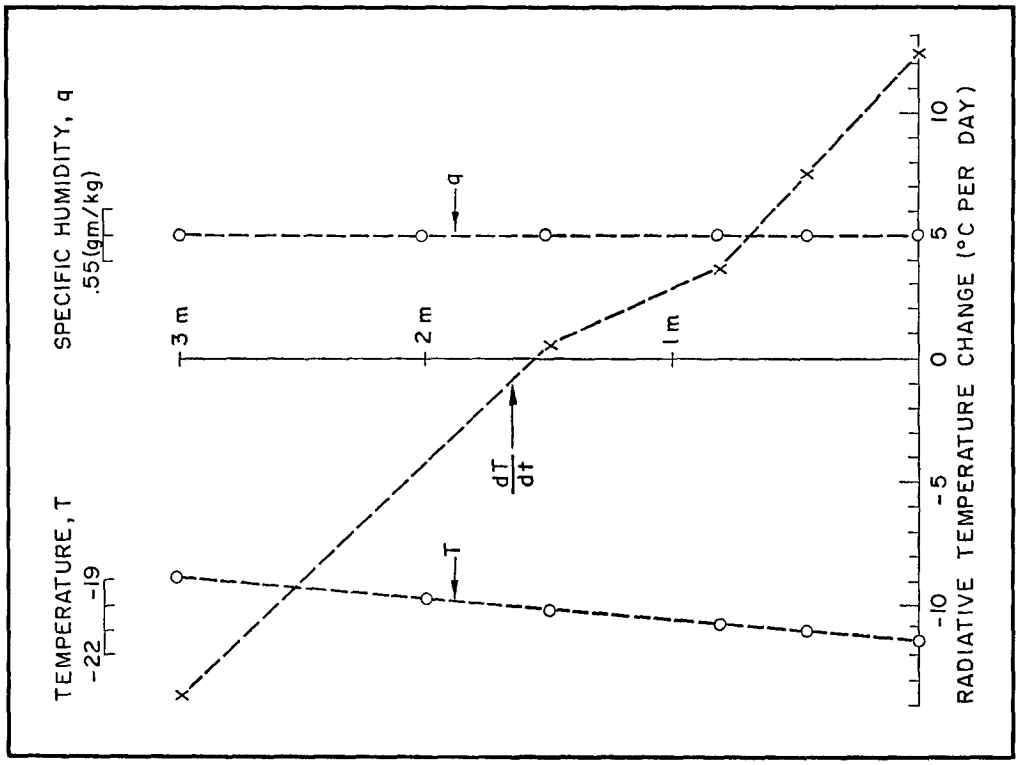

FIG. 3b. Radiative cooling in the lower levels of a continental polar air mass.

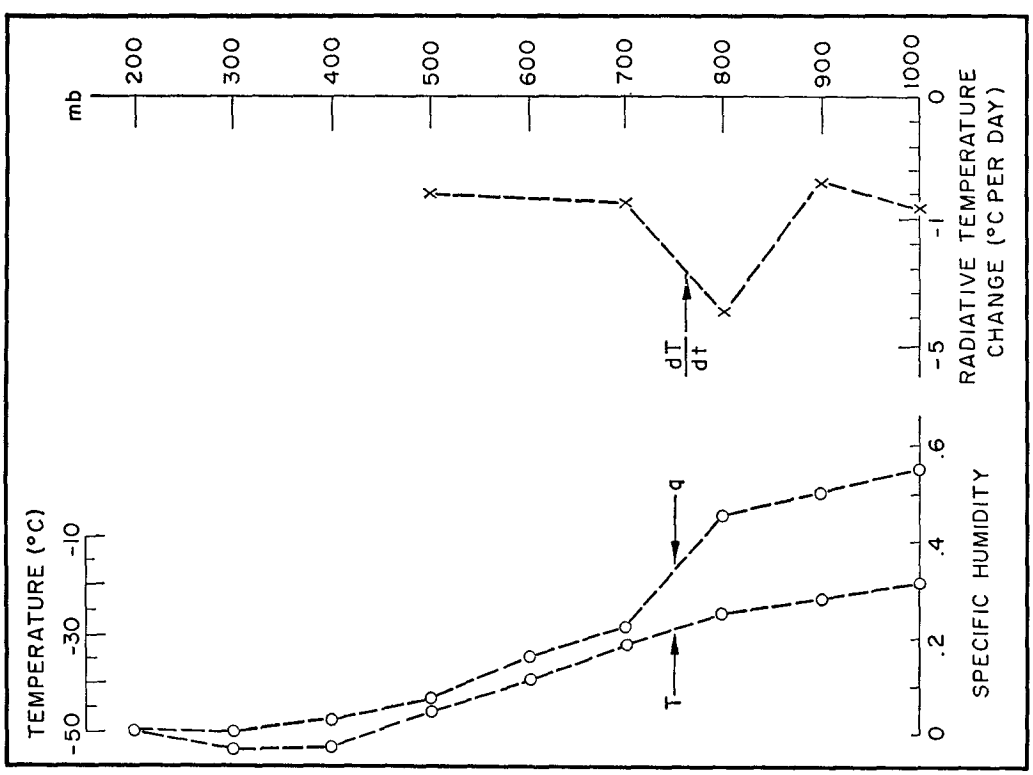

FIG. 3a. Radiative temperature change in a continental polar air mass.

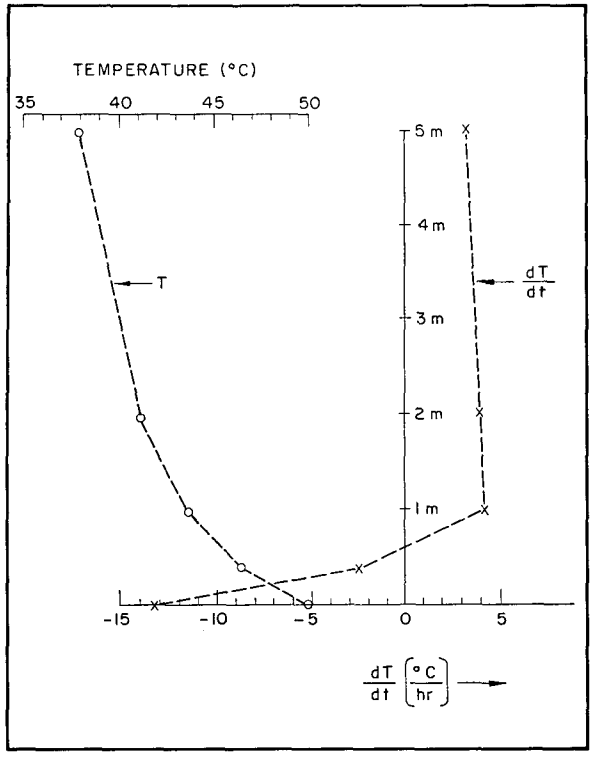

FIG. 4a. Radiative temperature change in the lower layers of a continental tropical air mass, assuming a smooth temperature distribution.

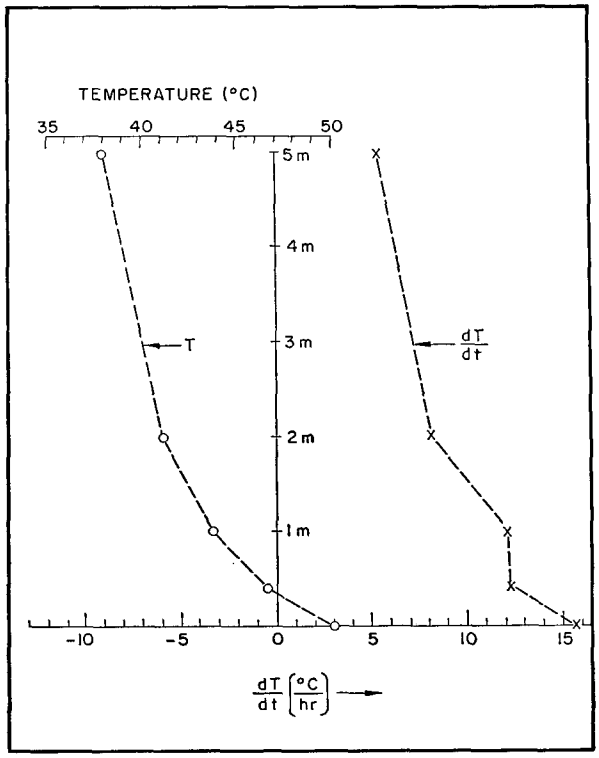

FIG. 4c. Radiative temperature change in the lower layers of a continental tropical air mass, assuming a smooth temperature distribution and a 10C interface difference $(T_G - T_0) = 10C$.

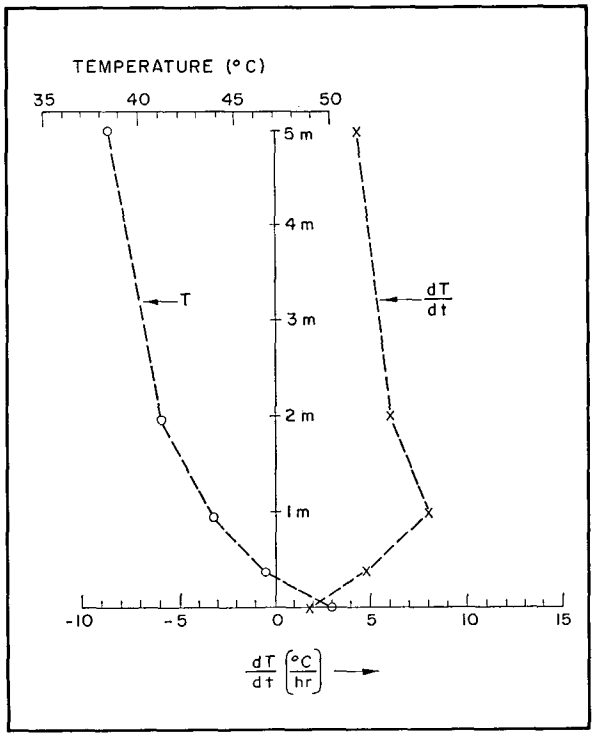

FIG. 4b. Radiative temperature change in the lower layers of a continental tropical air mass, assuming a smooth temperature distribution and a 5C interface difference $(T_G - T_0) = 5C$.

Geophysical Year, 1960). Above 850 mb, observed temperature and humidity data were used. Below this level, the sounding was modified to eliminate the nocturnal inversion. The layer from the surface to 50 m was assumed to have a relative humidity of 2 per cent, a reasonable value. Upper level humidity data reveal no clouds present. Due to extremely small optical depths involved, an investigation of this type would not be possible using Brooks' tables or commonly used radiation charts.

The smooth decrease of temperature with height in Fig. 4a results in strong radiative cooling below 40 cm and subsequent warming above 40 cm. The strong cooling observed in the air overlying the surface will oppose a superadiabatic lapse rate often observed.

In Fig. 4b, an interface discontinuity of 5C was introduced. The influence of the flux from the warmer surface removes the strong radiative cooling and changes it to heating. The effect of this term is perceptible through the 5-m level. In Fig. 4c, an interface discontinuity of 10C was assumed. Very strong heating through the lower 5 m is now apparent. Thus, temperature discontinuities at the surface are essential in explaining the existence of strong superadiabatic layers which are often observed.

5. Conclusion

It is felt that the use of this revised slope table will improve the accuracy of radiative flux divergence calculations. In addition, this table contains a very useful and physically reasonable extension toward shorter path lengths and eliminates extrapolation and recomputations of slopes that are required if Brooks' data are to be used for micrometeorological purposes. It is shown that the interface temperature is extremely important for any micrometeorological study. Radiative temperature changes obtained by Brooks and others are fairly realistic, as must be inferred from this investigation. Radiative warming is observed in the extreme lower layers of a continental polar air mass. An interface temperature discontinuity in a dry tropical air mass explains superadiabatic lapse rates often observed.

Recommendation. More and better low level humidity and temperature data must be collected in conjunction with low level flux divergence measurements. This will provide a check on slope values for very shallow optical depths.

REFERENCES

Brooks, D. L., 1950: A tabular method for the computation of temperature change by infrared radiation in the free atmosphere. *J. Meteor.*, **7**, 313–321.

Elsasser, W. M., 1942: Heat transfer by infrared radiation in the atmosphere. *Harvard Meteor. Studies, No. 6,* Cambridge, Harvard University Press, 107 pp.

——, with M. F. Culbertson, 1960: Atmospheric radiation tables. *Meteor. Monogr.*, **4**, No. 23, 43 pp.

Hales, J. V., W. Zdunkowski and D. Henderson, 1963: A study of the physical, thermodynamical, and dynamical causes of low ceiling and visibilities. Intermountain Weather, Inc., Final Report, Contract AF 19(604)-7333.

——, —— and ——, 1964: Flux divergence in a multi-component atmosphere. Intermountain Weather, Inc., in preparation for publication.

International Geophysical Year World Data Center A, 1960: I.G.Y. meteorological data on microcards. *I.G.Y. General Report Number 9,* National Research Council,

Kuhn, J. V., 1963: Radiometersonde observations of infrared flux emissivity of water vapor. *J. Appl. Meteor.*, **2**, 368–378.

Möller, F., 1951: Thermodynamics of clouds. *Compendium of Meteorology,* Boston, Amer. Meteor. Soc., 199–206.

——, and W. Zdunkowski, 1962: Computational methods of long wave radiation. Meteorologisches Institut der Universitat München. Technical Report, Contract AF 61(052)-493.

Petterssen, S., 1940: *Weather Analysis and Forecasting.* New York City, McGraw-Hill Book Co., Inc., 169–180.

Suomi, V. E., and P. M. Kuhn, 1958: An economical net radiometer. *Tellus,* **10**, 160–163.

U. S. Air Force, 1st Weather Wing, 1955: Far East climatology of jet stream. *Special Study 105–1,* Department of the Air Force.

Yamamoto, G., 1952: On a radiation chart. *Scientific Reports, Tôhoko University, Series 5, Geophys.*, **4**, 1.

Zdunkowski, W., 1963: Langwellige Strahlungswirkungen einer hochgelegenen Dunstschicht in der Atmosphäre. *Gerlands Beitr. Geophys.*, **2**, 103–126.